ANNALS of the ORADEA UNIVERSITY.
Fascicle of Management and Technological Engineering, Volume IX (XIX), 2010, NR2

ELASTIC PLASTIC NON-CONFORMING CONTACT MODELING PART I: ALGORITHM OVERVIEW

FRUNZA Gheorghe, SPINU Sergiu
University "Stefan cel Mare" of Suceava, ROMANIA
sergiu.spinu@fim.usv.ro

Keywords: elastoplasticity, reciprocal theorem, residual state, elastic part, iteration, plastic strain increment

Abstract: A fast algorithm for elastic-plastic non-conforming contact simulation is presented in this paper. As plasticity is history dependent, namely current state depends upon all pre-existing states, the algorithm is incremental. The plastic strain increment is determined using an universal integration algorithm for isotropic elastoplasticity proposed by Fotiu and Nemat-Nasser. Betti's reciprocal theorem is employed to assess surface normal displacement and stress state in an elastic half-space in the presence of plastic strains. Elastic-plastic normal contact problem is solved iteratively based on the relation between pressure distribution and plastic strain, until the latter converges.

1. INTRODUCTION

While the elastic response of a material subjected to load application is reversible, plasticity theory describes the irreversible behavior of the material in reaction to loading beyond the limit of elastic domain. The transition between elastic and plastic deformation is marked by the yield strength of the softer material.

The modern approach in modeling elastic-plastic contact is based on the algorithm originally proposed by Mayeur, [11], for the elastic-plastic rough contact. However, his works was limited to two-dimensional contact, as influence coefficients were derived for this case only. Generalization to three-dimensional contact was performed by Jacq, [7], and by Jacq et al. [8], who advanced a complete semi-analytical formulation for the elastic-plastic contact.

The algorithm was later refined by Wang and Keer, [15], by improving the convergence of residual and elastic loops. The main idea of the newly proposed Fast Convergence Method (FCM) is to use the convergence values for the current loop as initial guess values for the next loop. This approach reduces the number of iterations if the loading increments are small. Wang and Keer used two-dimensional Discrete Convolution Fast Fourier Transform (DCFFT), [9], to speed up the computation of convolution products.

Jacq's influence coefficients for residual stress computation were based on the problem decomposition advanced by Chiu [4,5]. An alternative approach was proposed by Liu and Wang, [10], who also suggested that three-dimensional DCFFT can be used in a hybrid algorithm incorporating convolution and correlation with respect to different directions. Their Discrete Correlation Fast Fourier Transform (DCRFFT) algorithm uses convolution theorem to assess correlation, by substituting one term of the convolution product by its complex conjugate.

Nélias, Boucly and Brunet, [12], improved the convergence of the residual loop, by assessing plastic strain increment with an algorithm for integration of elastoplasticity constitutive equations proposed by Fotiu and Nemat-Nasser, [6], as opposed to existing formulation, based on Prandtl-Reuss equations, [8]. As stated in [12], this results in a decrease of one order of magnitude in the CPU time.

Influence of a tangential loading in elastic-plastic contact was assessed by Antaluca, [1]. However, only isotropic hardening was considered in existing models. Kinematic hardening was added by Chen, Wang, Wang, Keer □i Cao, [3], who advanced a three-dimensional numerical model for simulating the repeated rolling or sliding contact of a rigid sphere over an elastic-plastic half-space.

2. ELASTIC-PLASTIC CONTACT ALGORITHM OVERVIEW

Since the works of Mayeur, [11] and Jacq, [7], Betti's reciprocal theorem is used in elastic-plastic contact modeling to assess surface normal displacement and stress state in an elastic half-space in the presence of plastic strains. Resulting equations suggest elastic-plastic contact problem split in an elastic and a residual part. The elastic part comprises the static force equilibrium, interference equation, and complementarity conditions, while the residual part expresses the plastic strain increment and plastic zone contribution to surface normal displacement and stress state in the elastic-plastic body. However, the two subproblems cannot be solved independently, as residual displacement, computed in the residual subproblem, enters interference equation in the elastic part, while contact stress, assessed in the elastic subproblem, is needed to find the plastic strain increment in the residual part.

Analytical resolution of resulting equations is available for neither elastic, nor residual part, as integration domains, namely boundary region with tractions and plastic strain volume respectively, not known a priori, are arbitrarily shaped. Therefore, numerical approach is preferred.

The principle of numerical approach consists in considering continuous distributions as piece-wise constant on the cells of a three-dimensional grid imposed in a volume enveloping integration domains. Continuous integration in the continuous model of the elastic-plastic contact model is replaced by multi-summation of elementary cells contributions, known from the influence coefficients or the Green functions. As these multi-summation operations are in fact convolution and/or correlation products, spectral methods are applied to speed up the computation.

The numerical model of the elastic part is obtained from that corresponding to a normal elastic contact problem completed with the residual term, namely the residual displacement, which is superimposed into the interference equation. Consequently, the elastic subproblem can be treated as an elastic contact problem with a modified initial contact geometry. The most efficient solver is based on the conjugate gradient algorithm advanced by Polonsky and Keer, [13], tweaked with the DCFFT technique for convolution evaluation.

In the same manner, the residual part is reformulated numerically, by imposing digitized plastic strain distribution and finite load increments. Plastic strain contribution to normal surface displacement is expressed as a two-dimensional convolution, computed by a two dimensional DCFFT. The problem of residual stresses induced in the half-space by an arbitrary distribution of inelastic deformations is solved following a method originally suggested by Chiu [4,5]. The hybrid three dimensional spectral algorithms newly proposed by Spinu, [14], result in a dramatic decrease in computational effort.

The algorithm proposed for simulation of elastic-plastic non-conforming contact with isotropic behavior is based on three levels of iteration.

The innermost level, which assesses plastic strain increment, corresponds to the residual part, and has a fast convergence, as described in the following section. The second level adjusts contact pressure and residual displacement in an iterative approach specific to elastic contact problems with modified contact geometry.

The outermost level is related to the fact that, unlike elastic solids, in which the state of strain depends on the achieved state of stress only, deformation in a plastic body depends on the complete history of loading. This level applies the load incrementally, until the imposed value is reached.

The algorithm for solving one loading step in the elastic-plastic normal contact problem is summarized in Fig. 1.

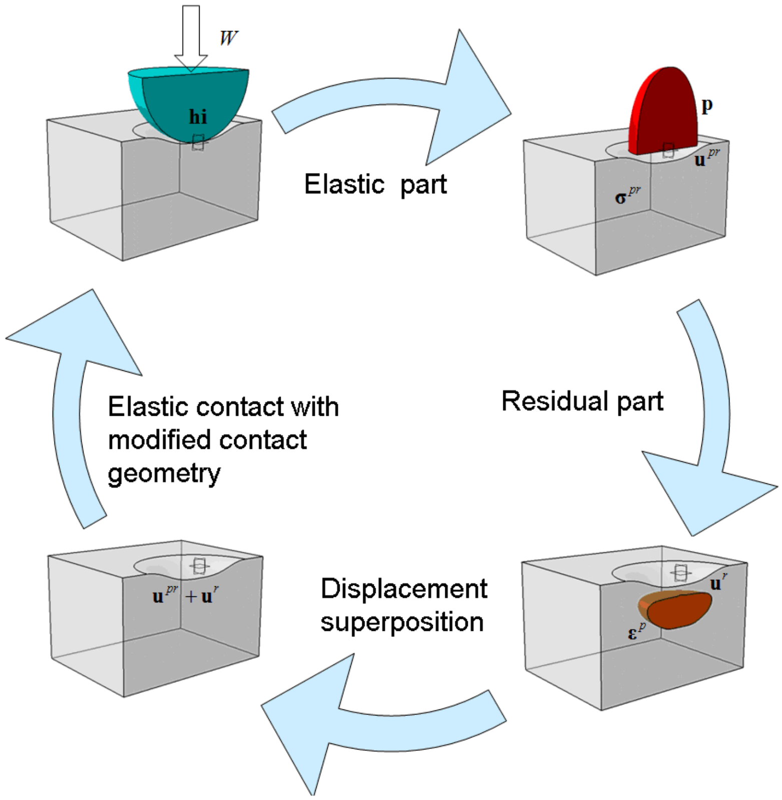

Figure 1. Elastic -plastic algorithm

Firstly, the elastic problem with modified contact geometry **hi** is solved, yielding contact area and pressure distribution **p**. The latter can be used to assess elastic displacement field $\mathbf{u}^{pr}$ and stress field $\boldsymbol{\sigma}^{pr}$. These terms represent the elastic part of displacement and stress, namely that part that is recovered once loading is removed. The stresses induced by pressure are used in the residual subproblem, to assess plastic strain increment. The algorithm, based on a method originally proposed by Fotiu and Nemat-Nasser, [6], is discussed in detail in the following section. The computed plastic strain increment is used to adjust the achieved plastic zone $\boldsymbol{\varepsilon}^{p}$. Once the volume with plastic strains is known, residual parts of displacement, $\mathbf{u}^{r}$, and of stresses, $\boldsymbol{\sigma}^{r}$, can be computed. As opposed to their elastic counterparts, terms $\mathbf{u}^{r}$ and $\boldsymbol{\sigma}^{r}$ express a potential state, that remains after contact unloading, if no plastic flow occurs during contact relief. The total displacement can then be computed, $\mathbf{u}^{pr}+\mathbf{u}^{r}$, thus imposing a new interference equation in the elastic subproblem. These sequences are looped until convergence is reached.

3. PLASTIC STRAIN INCREMENT

According to general theory of plasticity, plastic flow occurrence can be described mathematically with the aid of a yield function, assessing the yield locus in the multidimensional space of stress tensor components. If von Mises criterion is used to express stress intensity, this function can be expressed as:

$$f(e^{p})=\sigma_{VM}-\sigma_{Y}(e^{p}), \qquad (1)$$

where e^p denotes the effective accumulated plastic strain, $e^p = \sqrt{2\varepsilon_{ij}^p \varepsilon_{ij}^p / 3}$, and $\sigma_Y(e^p)$ is the yield strength function. The latter satisfy the relation for the initial yield strength σ_{Y0}:

$$\sigma_Y(0) = \sigma_{Y0}. \tag{2}$$

The following conditions must be met:

$$f \le 0;\ de^p \ge 0;\ f \cdot de^p = 0, \tag{3}$$

with conditions $f = 0$ and $de^p > 0$ corresponding to plastic flow.
For elastic-perfectly plastic materials, relation (2) is verified for any value of e^p. However, for metallic materials, more complex models of elastic-plastic behavior are used, as the isotropic, or the kinematic hardening laws. The isotropic hardening law of Swift, [2]

$$\sigma_Y(e^p) = B(C + e^p)^n, \tag{4}$$

with B, C and n material constants, is used in the current formulation.
According to flow rule, [11], plastic strain increment can be expressed as:

$$d\varepsilon_{ij}^p = de^p \frac{\delta f}{\delta \sigma_{ij}} = de^p \frac{3S_{ij}}{2\sigma_{VM}}, \tag{5}$$

where S_{ij} denotes the deviatoric stress tensor.
The algorithm used to derive the plastic strain increment was advanced by Fotiu and Nemat-Nasser, [6], who developed a universal algorithm for integration of elastoplasticity constitutive equations. As stated in [6], the algorithm is unconditionally stable and accurate for large load increments, as it takes into account the entire non-linear structure of elastoplasticity constitutive equations, which are solved iteratively, via Newton-Raphson numerical method, at the end of each loading step. The yield function f is linearized at the beginning of the load increment, by employing an elastic predictor. This places the state point far outside the yield surface $f = 0$, since elastic-plastic modulus is small compared to the elastic one. The return path to the yield surface is generated by the plastic corrector, via Newton-Raphson iteration. This approach, also referred to as elastic predictor - plastic corrector, is efficient when most of the total strain is elastic. In the fully plastic regime, which occurs usually after the elastic-plastic one, the plastic strain is predominant, thus the return path may require numerous iterations. Thus, linearization is performed by a plastic predictor, and return path with an elastic corrector.
A yield occurs when von Misses stress exceeds current yield stress, namely $f > 0$. The elastic domain expands or translates to include the new state point, namely to verify condition $f = 0$. The actual increment of effective accumulative plastic strain should satisfy equation of the new yield surface in the plastic zone:

$$f(e^p + \delta e^p) = 0. \tag{6}$$

Here, δe^p denotes the finite increment of effective plastic strain, as defined in [7]. Relation (6) can be considered as an equation in δe^p, which is solved numerically by

Newton -Raphson iteration. To this end, yield surface relation is linearized along plastic corrector direction:

$$f(e^p + \delta e^p) = f(e^p) + \delta e^p \frac{\partial f(e^p)}{\partial e^p} = 0\,, \tag{7}$$

yielding the plastic corrector:

$$\delta e^p = -f(e^p) \Big/ \frac{\partial f(e^p)}{\partial e^p} = f(e^p) \Big/ \left(\frac{\partial \sigma_Y(e^p)}{\partial e^p} - \frac{\partial \sigma_{VM}}{\partial e^p} \right). \tag{8}$$

For izotropic hardening, the derivate of equivalent von Mises stress with respect to effective accumulative plastic strain was derived by Nélias, Boucly and Brunet, [12], from the general equations presented in [6] for rate-dependent elastoplasticity:

$$\frac{\partial \sigma_{VM}}{\partial e^p} = -3G\,. \tag{9}$$

With these results, the following return-mapping algorithm with elastic predictor - plastic corrector can be formulated:

1. Acquire the state at the beginning of the loading step and impose the elastic predictor. For elastic-plastic contact problems, this translates to solving an elastic loop without imposing any residual displacement increment. Corresponding parameters are identified by an "a" superscript, as opposed to a "b" superscript, used to denote the state at the end of the load increment: $e^{p(a)}$, $\sigma_Y^{(a)} = \sigma_Y(e^{p(a)})$, $\sigma_{ij}^{(a)}$ $(\sigma_{ij}^{(a)} = \sigma_{ij}^{pr(a)} + \sigma_{ij}^{r(a)})$, $\sigma_{VM}^{(a)}$, $f^{(a)} = \sigma_{VM}^{(a)} - \sigma_Y^{(a)}$. These variables also represent the input for the Newton-Raphson iteration. Thus, by using superscripts to denote the Newton-Raphson iteration number, $e^{p(1)} = e^{p(a)}$, $\sigma_Y^{(1)} = \sigma_Y^{(a)}$, $\sigma_{ij}^{(1)} = \sigma_{ij}^{(a)}$, $\sigma_{VM}^{(1)} = \sigma_{VM}^{(a)}$, $f^{(1)} = f^{(a)}$.

2. Start the Newton-Raphson iteration. Compute the plastic corrector according to relations (8) and (9):

$$\delta e^{p(i)} = f^{(i)} \Big/ \left(\frac{\partial k(e^{p(i)})}{\partial e^{p(i)}} + 3G \right). \tag{10}$$

3. Use the plastic corrector to adjust model parameters:

$$\sigma_{VM}^{(i+1)} = \sigma_{VM}^{(i)} - 3G\delta e^{p(i)}; \tag{11}$$

$$e^{p(i+1)} = e^{p(i)} + \delta e^{p(i)}; \tag{12}$$

$$\sigma_Y^{(i+1)} = \sigma_Y(e^{p(i+1)}); \tag{13}$$

$$S_{ij}^{(i+1)} = \frac{\sigma_{VM}^{(i+1)}}{\sigma_{VM}^{(1)}} S_{ij}^{(1)}. \tag{14}$$

4. Verify if eq. (6) is verified to the imposed tolerance eps. If condition

$$\left|f^{(i+1)}\right| = \left|\sigma_{VM}^{(i+1)} - \sigma_{Y}^{(i+1)}\right| > eps \tag{15}$$

is satisfied, go to step 2. If else, convergence is reached, and the state point at the end of the loading step is described by the newly computed parameters: $e^{p(b)} = e^{p(i+1)}$, $\sigma_{VM}^{(b)} = \sigma_{VM}^{(i+1)}$, $S_{ij}^{(b)} = S_{ij}^{(i+1)}$.

5. Compute the plastic strain increment, according to Eq. (5):

$$\delta\varepsilon_{ij}^{p} = \left(e^{p(b)} - e^{p(a)}\right)\frac{3S_{ij}^{(b)}}{2\sigma_{VM}^{(b)}}. \tag{16}$$

This increment is used to update the plastic zone. The residual parts of displacement and of stress can then be computed, and superimposed to their elastic counterparts.

4. COMPUTATIONAL ADVANTAGES

The new algorithm for computation of plastic strain increment improves dramatically the speed of convergence for the residual subproblem. The existing formulation, advanced by Jacq et al., based on the Prandtl-Reuss algorithm, implies iteration of a tensorial parameter, namely the plastic strain increment, as opposed to the new algorithm, which iterates a scalar, namely the increment of effective accumulative plastic strain. Convergence of the Newton-Raphson scheme is reached after few iterations. As stated in [6], the method is accurate even for large loading increments.

Moreover, the classic algorithm is based on the reciprocal adjustment between plastic strain and residual stress increments. Consequently, at every iteration of the residual loop, it is necessary to express the residual stress increment. Its assessment implies superposition, with both source (integration) and observation domains being three-dimensional. Although three-dimensional spectral methods, [14], were applied to speed up the computation, the CPU time and memory requirements remain prohibitively high.

In the new algorithm, this dependence needs to be evaluated at every iteration of the elastic loop, after the plastic zone is updated with the new plastic strain increment. In other words, residual stress assessment is moved to an upper iterative level, resulting in increased computational efficiency. Consequently, with the same computational effort, a finer grid can be imposed in the numerical simulations, thus reducing the discretization error.

5. CONCLUSIONS

This paper summarizes an efficient algorithm for simulation of elastic-plastic point contacts. Computation of plastic strain increment is presented in detail. The plastic strain increment is determined in a fast convergent Newton-Raphson procedure which iterates a scalar, namely the effective accumulative plastic strain. The method, originally suggested by Fotiu and Nemat-Nasser, employs an elastic predictor, which places the stress point outside yield surface, and a plastic corrector, assessing the return path to the yield locus. The method is fats, stable and accurate even for large loading steps.

An additional advantage arises from moving residual stress computation to an upper iterative level.

Plastic strain modifies contact pressure by superimposing induced residual surface displacement into the initial contact geometry. Contact pressure, in its turn, contributes to the subsurface stress state, responsible for plastic zone development. Consequently, the model is solved iteratively based on the relation between pressure distribution and plastic strain, until the latter converges.

REFERENCES

[1] Antaluca, E., (2005), *Contribution a l'étude des contacts élasto-plastiques - effet d'un chargement normal et tangentiel*, Ph.D. Thesis, INSA Lyon, France.
[2] Boucly, V., Nélias, D., and Green, I., (2007), *Modeling of the Rolling and Sliding Contact Between Two Asperities*, ASME J. Tribol., 129, pp. 235 - 245.
[3] Chen, W. W., Wang, Q. J., Wang, F., Keer, L. M., and Cao, J., (2008), *Three-Dimensional Repeated Elasto-Plastic Point Contacts, Rolling, and Sliding*, ASME J. Tribol., 75, pp. 021021-1 - 021021-12.
[4] Chiu, Y. P., (1977), *On the Stress Field Due to Initial Strains in a Cuboid Surrounded by an Infinite Elastic Space*. ASME J. Appl. Mech., 44, pp. 587–590.
[5] Chiu, Y. P., (1978), *On the Stress Field and Surface Deformation in a Half Space with Cuboidal Zone in Which Initial Strains Are Uniform*. ASME J. Appl. Mech., 45, pp. 302–306.
[6] Fotiu, P. A., and Nemat-Nasser, S., (1996), *A Universal Integration Algorithm for Rate-Dependant Elastoplasticity*, Comput. Struct., 59, pp. 1173–1184.
[7] Jacq, C., (2001), *Limite d'endurance et durée de vie en fatigue de roulement du 32CrMoV13 nitruré en présence d'indentations*, Ph.D. Thesis, INSA Lyon, France.
[8] Jacq, C., Nelias, D., Lormand, G., and Girodin, D., (2002), *Development of a Three-Dimensional Semi-Analytical Elastic-Plastic Contact Code*. ASME J. Tribol., 124, pp. 653–667.
[9] Liu, S. B., Wang, Q., and Liu, G., (2000), *A Versatile Method of Discrete Convolution and FFT (DC-FFT) for Contact Analyses*. Wear, 243 (1–2), pp. 101–111.
[10] Liu, S. Wang, Q., (2005), *Elastic Fields due to Eigenstrains in a Half-Space*. ASME J. Appl. Mech. 72, pp. 871–878.
[11] Mayeur, C., (1995), *Modélisation du contact rugueux élastoplastique*. Ph.D. Thesis, INSA Lyon, France.
[12] Nélias, D., Boucly, V., and Brunet, M., (2006), *Elastic-Plastic Contact Between Rough Surfaces: Proposal for a Wear or Running-in Model*, ASME J. Tribol., 128, pp. 236 - 244.
[13] Polonsky, I. A., and Keer, L. M., (1999), *A Numerical Method for Solving Rough Contact Problems Based on the Multi-Level Multi-Summation and Conjugate Gradient Techniques*. Wear, 231(2), pp. 206–219.
[14] Spinu, S., (2009), *Contributions to the Solution of the Elastic-Plastic Normal Contact Problem*, (in Romanian), PhD Thesis, University of Suceava, Romania.
[15] Wang, F., and Keer, L. M., (2005), *Numerical Simulation for Three Dimensional Elastic-Plastic Contact With Hardening Behavior*. ASME J. Tribol., 127, pp. 494–502.